

Conductivity Evaluation of Horizontal Wells in Coalbed Methane Reservoirs: Applicability of Micromaterial Tracer Testing Technology

Wei Zhang,* Xiaoguang Sun, Lingbo Wang,* Yongchen Li, Gang Zhao, and Wenhui Meng

Cite This: *ACS Omega* 2023, 8, 1131–1139

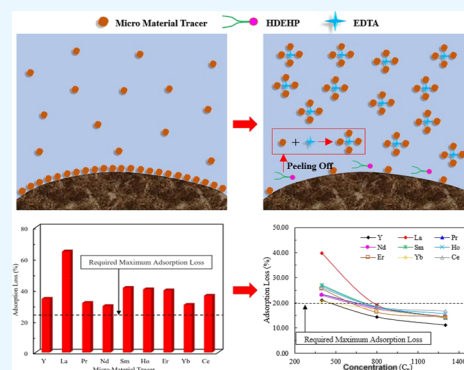
Read Online

ACCESS |

Metrics & More

Article Recommendations

ABSTRACT: Horizontal well-staged fracturing technology is widely used in the exploitation of coalbed methane reservoirs. Most coalbed methane wells have little or no flowback fluid after fracturing due to strong adsorption in the reservoir. The fracture conductivity of each fracturing interval can only be evaluated in the water drainage and gas production stage. Traditional chemical tracer monitoring technologies are risky to operate and do not provide accurate qualitative measurements. The potential applicability of trace material tracer testing technology in coalbed methane reservoirs has theoretical and practical significance, as does establishing a set of fracturing tracer technologies (e.g., reagent systems, construction schemes, detection interpretation) suitable for coalbed methane horizontal wells. Geological, laboratory, and field test data are used in this study to preliminarily resolve the trace material tracer adsorption problem in the coalbed by improving the chemical agent formula. The proposed method is applied to determine the conductivity of a fractured section in a coalbed methane well.



1. INTRODUCTION

The over-consumption of conventional oil and gas resources has created urgent demand for new energy, driving the exploration and development of unconventional oil and gas resources. Unconventional oil and gas reservoir development generally requires fracturing for industrial productivity.^{1–4} There has been rapid and extensive development to date of unconventional oil and gas resources such as coalbed methane, shale gas, tight oil, and tight gas. Hydraulic fracturing can convert the original radial seepage fluid flow in the well into linear for the purpose of stimulation. However, there are unresolved problems regarding the fracturability of the formation and the ability to form complex fracture network systems after fracturing.^{5–9}

After the large-scale fracturing of unconventional oil and gas reservoirs, including coalbed methane reservoirs, it is necessary to effectively evaluate the fracturing effect of horizontal wells, monitor the fracture conductivity of each section, and predict the productivity of each section. These evaluations are an important prerequisite for an effective, efficient production system. At present, there is a lack of sufficiently advanced technologies for productivity monitoring in individual horizontal well sections.^{10–13} Compared with other monitoring technologies, fracturing tracer monitoring technology shows obvious advantages in evaluating fracturing flowback effects and fracture conductivity.¹⁴ The tracer monitoring method involves supplying various rare-earth element tracers in different fracturing intervals via fracturing fluid; after fracturing, the tracers return with the formation fluid at a

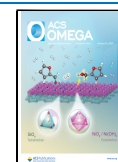
different level of pressure than production. The output of the tracer in each fracturing interval differs when it is discharged to the surface due to variations in the fracturing effects and physical properties of each oil layer. Flowback effect can be examined through variations in the concentration of the tracer in the flowback fluid, then the production capacity of each section can be predicted accordingly.^{15,16}

The liquid production profile testing technology of horizontal wells differs substantially from traditional vertical well testing technology. In vertical wells, devices can be lifted and lowered directly by the weight of the tool or with an added heavy rod. In horizontal wells, external force is applied to send the tool to the target layer.^{17,18} There are five common horizontal wells production profile testing technologies in use presently: Coiled tubing transportation, specially made hard cable transportation, surface hydrodynamic transportation, underground crawler transportation, and fiber optic sensor transportation.^{19,20} However, these technologies can only be applied during shutdown. The cable is exposed in the oil casing annulus, where it is easily damaged. Other shortcomings include anti-rotation and anti-cable accumulation during

Received: October 11, 2022

Accepted: December 7, 2022

Published: December 16, 2022



construction, the high cost of optical fiber sensors, and difficulty in removing the test tool from the well after the test is complete. Conventional horizontal well liquid production profile test methods do not satisfy the requirements for liquid production profile testing in coalbed reservoirs.

The tracers used in traditional tracer monitoring methods mainly include chemical tracers, which necessitate large dosages despite their relatively low precision, as well as radioisotope tracers and nonradioactive (stable) isotope tracers. Although the traditional tracer monitoring technology performs well in oilfield water injection fracturing development, coal is a porous medium with fractal characteristics and strongly adsorbs tracers.²¹ The adsorption capacity of coal is related to its deformation structure; furthermore, various deformation properties and degrees give tectonic coal different levels of adsorption capacity. The pore structure properties of coal, including the pore volume, specific surface area, pore size distribution (PSD), and pore shape affect its adsorption as well.^{22–24} Considering these characteristics of coal reservoirs, traditional tracer monitoring technology cannot be applied to the evaluation of their horizontal well production profiles. The advantages and disadvantages of traditional tracer monitoring technology are summarized in Table 1.

Fourth-generation tracer technologies are considered to be safe, stable, precise, various in formulation, and administrable in relatively low dosages.^{31–33} The advantageous characteristics of trace-material tracers render tracer monitoring technology applicable to the staged testing of horizontal wells in coal reservoirs.

The trace-material tracer is the most advanced type of tracer monitoring technology available currently and has been successfully applied in the oilfield water injection development.^{34–36} However, trace substance tracer monitoring technology is rarely used in coal reservoirs. Whether this monitoring technology can be designed to overcome the strong adsorption characteristics of coal and successfully applied to the liquid production profile test of horizontal wells in coal reservoirs still needs further research. Further details regarding coal reservoir tracer monitoring technology tracer selection can be found in the *Oilfield water injection chemical tracer selection method* (SY/T 5925-2012).³⁷

In summary, the conventional horizontal well production profile test method and traditional chemical tracer monitoring technologies do not apply to horizontal well staged fracturing tests in coal reservoirs. Trace substance tracer monitoring technology is a new approach to staged fracturing testing in coalbed methane horizontal wells. In this work, we examine the feasibility, compatibility, thermal stability, mutual interference, static adsorption, and other properties of tracers in coalbed methane reservoirs. We also investigate whether the tracer meets the conditions for effective tracer monitoring technology in the staged fracturing of coalbed methane reservoirs.

2. RESULTS AND DISCUSSION

2.1. Tracer Stability, Compatibility, and Interference Test Results. The simulated coal seam temperature is 43 °C. A compatibility test of lanthanide tracer solution, formation water, and fracturing fluid solution was carried out according to the industry test standard. The results show a light transmittance over 90%, demonstrating good compatibility among the selected tracers, formation water, and fracturing fluid.

Table 1. Advantages, Disadvantages, and Applications of Traditional Tracer Monitoring Technology

tracer monitoring technology	tracers used	advantages	disadvantages	oilfield application
chemical tracer monitoring technology ^{25,26} (first generation)	inorganic salts, halogenated hydrocarbon fluorescent dyes, alcohols	diverse, easy to detect	large dosage, partial poisoning, poor precision (10^{-9} – 10^{-6} kg/L)	commonly used before 2015
radioisotope tracer monitoring technology ^{27,28} (second generation)	neon-containing compounds ^{12}C , ^{13}C , ^{15}C , ^{18}O	less dosage, easy to detect	strict operation, safety hazards	not commonly used
stable isotopes tracer detection technology ^{29,30} (third generation)		nonradioactive, easy to detect	fewer types, high cost, complex detection methods (atom reactor activation, neutron activation method measurement)	not commonly used

“Interference” in this context refers to the phenomenon whereby the spectra of elements overlap during a test, rendering elements undetectable or as doubled concentrations.³⁸ In the layered fracturing construction stage of horizontal wells, the types of trace tracers added in each fracturing section are different. Eventually, however, various tracers are mixed in the flowback process. To ensure accuracy of the final analysis, it is necessary to ensure that there is no interference between the selected tracers. Ultrapure water was used to prepare the selected nine trace substance tracers each into a 200 mg/L solution. Liquid chromatography was applied to test the mixed solution for any interference between various trace substance tracers. The results are shown in Figure 1.

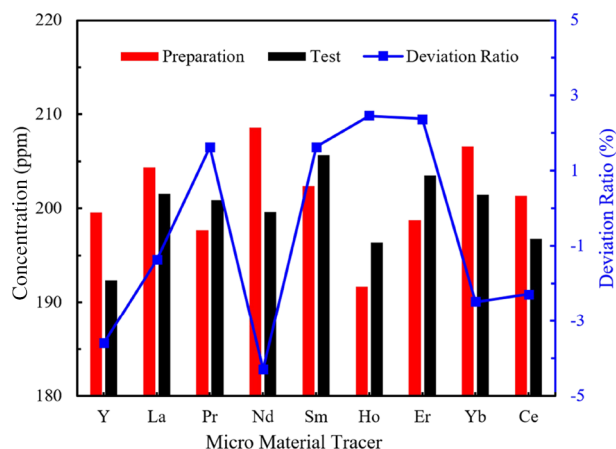


Figure 1. Interference experiment results.

As shown in Figure 1, the nine lanthanide metal elements in the mixed solution are close to the designated concentration with an error below 5% (which can be attributed to the experimental error). In effect, there is no interference between the nine trace material tracers. Therefore, these nine lanthanide metal elements can be used as tracers to mark fracturing fluids in different intervals.

2.2. Tracer Minimum Detection Limit Determination Results. The lowest detection limits of nine trace substance tracers measured by an ICP-MS/Agilent 7900 inductive coupled plasma mass spectrometer are shown in Table 2. The minimum detectable concentrations of the nine tracers are represented here by C_n ($n = 1, 2, 3, 4, 5, 6, 7, 8,$ and 9).

Table 2. Minimum Detection Limits of Nine Elements

element	Y	La	Pr	Nd	Sm	Ho	Er	Yb	Ce
lowest detection (mg/m ³)	10	20	80	90	20	50	50	20	80

2.3. Adsorption Loss of Micromaterial Tracers on Coal. Coal has strong adsorption capacity, as discussed above, where the material entered is quickly adsorbed on its porous surface. In order to study the adsorption capacity of coal to the micromaterial tracer, nine micromaterial tracers were tested on coal to observe their adsorption, as shown in Figure 2. The concentration of the micromaterial tracer used is 800 C_n and the corresponding concentration test results are listed in Table 3. The adsorption loss dynamics of micromaterial tracers are shown in Figure 3.

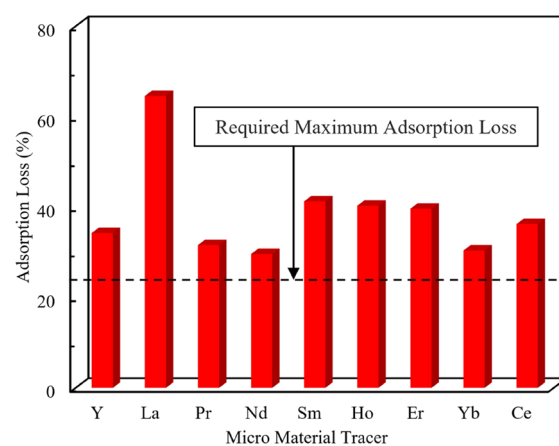


Figure 2. Adsorption loss of the micromaterial tracer (800 C_n).

The micromaterial tracer is widely used in oilfield dynamic characterization because of its low adsorption loss on rock surfaces. However, due to the special nature of coal, the adsorption loss of micromaterial tracers in the core porous surface is extremely high. As shown in Figure 2, the adsorption loss of the nine micromaterial tracers exceeds the maximum adsorption loss required for field applications. The adsorption loss of La, for example, is as high as 64.5%. The adsorption loss of Nd is the smallest among them but still reaches 29.7%.

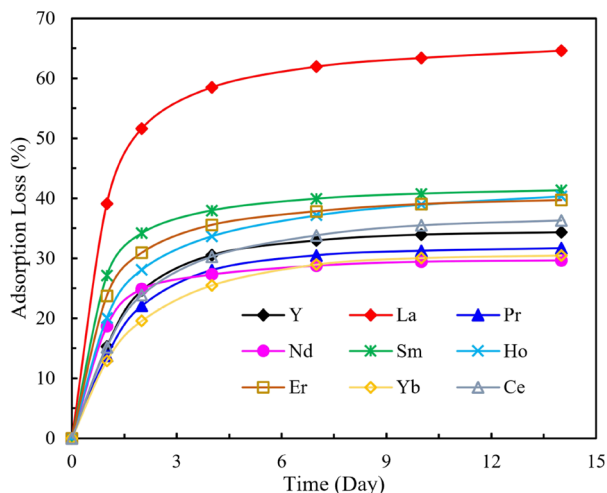
As shown in Figure 3, the adsorption kinetics further show that the adsorption of trace material tracers in coal is mainly concentrated on the first day. Therefore, when micromaterial tracers are applied to the coal reservoir, they are displayed only near the well area due to the rapid adsorption and high adsorption loss. The concentrations of micromaterial tracers decrease rapidly as they flow into the core porous media to the point that they are barely visible in the production well or are present at even lower levels than the minimum display concentration; thus, they cannot be utilized as tracers. It is necessary to add a certain amount of additives in water solution to inhibit the adsorption of coal before tracers can be applied.

2.4. Desorption of Micromaterial Tracers on Coal.
2.4.1. Desorption Mechanism for Micromaterial Tracers on Coal. A given micromaterial tracer exists in the strata in a manner dispersed over the surfaces of other rock minerals. During micromaterial tracer mineral development, HDEHP can be used as an extractant to peel the material from the rock surface to achieve efficient development. EDTA also exerts a complexation effect on micromaterial tracers under alkaline conditions, causing the tracers to form aggregates. EDTA, HDEHP, and NaOH were used together in this study to effectively inhibit micromaterial tracer adsorption in the coal surface (Figure 4). The optimal concentration observed in the test is EDTA (0.01%) + HDEHP (0.001%) + NaOH (0.00002%).

The EDTA + HDEHP + NaOH system successfully reduces micromaterial tracer adsorption in the coal surface in two main ways. First, in the solution containing EDTA + HDEHP + NaOH system, most micromaterial tracer molecules are distributed in an aqueous solution in the form of a complex, which reduces adsorption in the coal surface. Second, micromaterial tracer adsorbed in the coal surface is peeled off under the action of HDEHP.

Table 3. Test Results of Actual Element Concentration in Mixed Solution

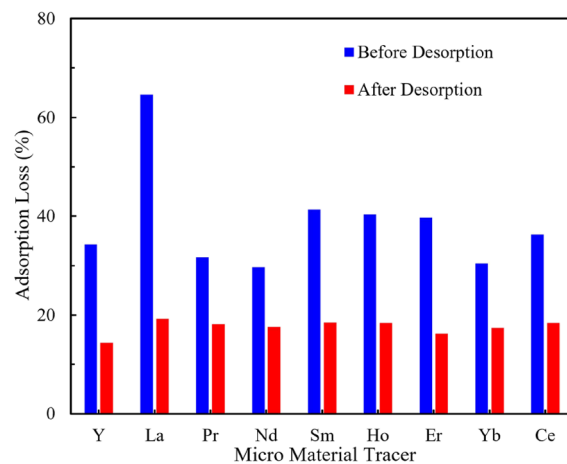
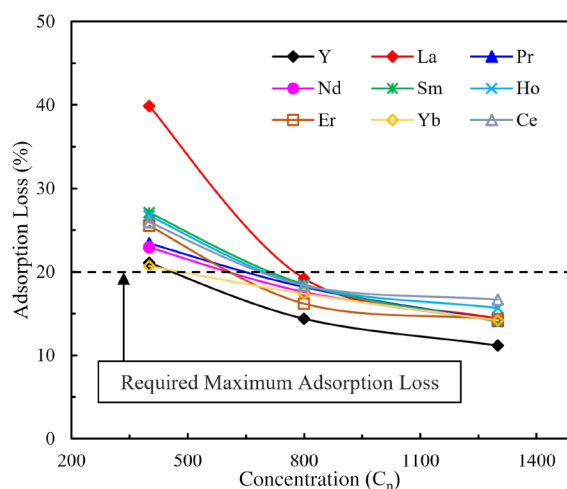
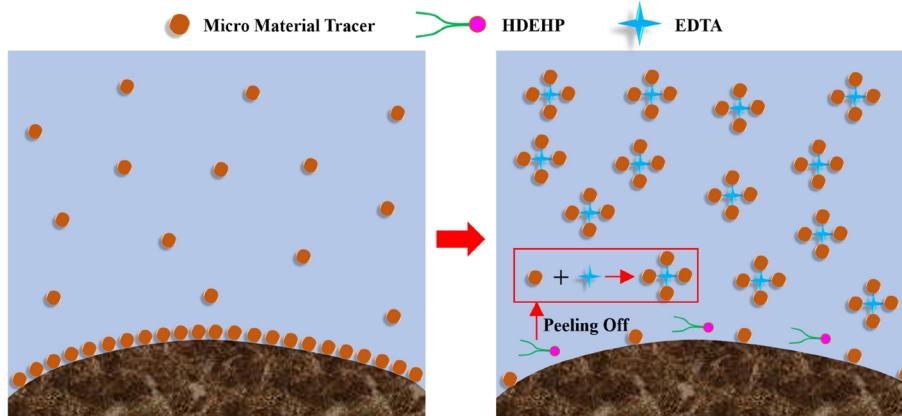
theoretical concentration	Y (mg/L)	La (mg/L)	Pr (mg/L)	Sm (mg/L)	Ho (mg/L)	Er (mg/L)	Nd (mg/L)	Yb (mg/L)	Ce (mg/L)
800 C_n	6.029	18.760	57.980	15.589	40.030	42.400	65.339	17.169	63.237

**Figure 3.** Adsorption dynamic of the micromaterial tracer (800 C_n).

2.4.2. Desorption Effect for Micromaterial Tracers on Coal. To verify the desorption effect of the EDTA + HDEHP + NaOH system on micromaterial tracers, we measured adsorption loss as shown in Figure 5. We find that after adding EDTA + HDEHP + NaOH, the adsorption loss of all nine micromaterial tracers was significantly reduced to less than 20%. The desorption capacity for La is the strongest, as adsorption loss decreased from 64.5 to 19.2%. The adsorption loss of Y is only 14.3%. Thus, the EDTA + HDEHP + NaOH system has a strong inhibitory effect on the adsorption capacity of micromaterial tracers in coal surfaces.

Figure 6 shows the adsorption loss of different micromaterial trace concentrations in coal under the same desorption system conditions. Adsorption loss decreases as the concentration increases. However, when the concentration is higher than 800 C_n , the decrease in adsorption loss decelerates but still satisfies field application requirements. The recommended concentration of the micromaterial tracer is 800 C_n .

2.5. Field Application. **2.5.1. Distribution of Horizontal Wells.** The distribution of existing horizontal wells in the B8–3 block is shown in Figure 7. The spacing between horizontal

**Figure 5.** Adsorption loss of micromaterial tracer before and after desorption (800 C_n).**Figure 6.** Adsorption loss of micromaterial tracers at different concentrations.**Figure 4.** Desorption mechanism for micromaterial tracer on the coal rock surface.

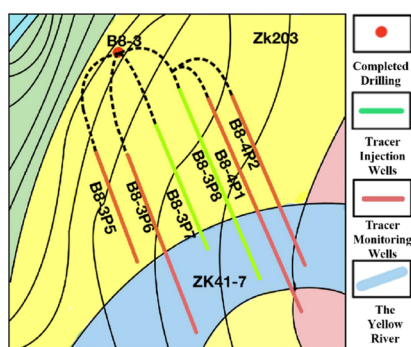


Figure 7. Existing well location distribution in the B8-3 block.

wells in this block is between 300 and 330 m. As shown in the figure, Well B8-3P7 and Well B8-3P8 are tracer injection wells; Well B8-3P5, Well B8-3P6, Well B8-4P1, and Well B8-3P2 are adjacent tracer monitoring wells. The B8-3P7 well and its corresponding monitoring adjacent well, and B8-3P8 well and its corresponding adjacent well, are located in two respective layers. The B8-3P7 well and its adjacent well are located in the 4 + 5[#] reservoir. The B8-3P8 well and its adjacent well are located in 8 + 9[#] reservoir.

2.5.2. Dosage of Tracers and Chemical Agents. The main principle of determining the necessary dosage of a tracer is to ensure the accuracy and reliability of evaluation data while also considering the economic input. Various possible influencing factors should be considered, and a certain margin should be reserved. The factors for determining dosages include the detection limit of the tracer element device in the fracturing fluid system, the fracturing construction scale (e.g., fracturing construction volume, the number of fracturing sections), the possible invasion of formation water, the maximum solubility of tracer compounds, and the discharge capacity of the tracer dosing pump.

The final dosing concentration of the tracer was determined here according to the fracturing construction scale (fracturing construction volume, number of fracturing sections), the maximum solubility of the tracer compound, and the discharge capacity of the tracer dosing pump. The dosage of tracer compound was determined according to the dosage concentration of the tracer and the total amount of the fracturing tracer.

We calculate tracer dosage as shown in eqs 1–3.

$$M = \mu C_n V_T \quad (1)$$

$$V_E = V_T / N \quad (2)$$

$$T = V_E / P_T \quad (3)$$

C_n , minimum detection limit concentration of the tracer, mg/m³; μ , empirical coefficient considering formation water intrusion and coal seam adsorption; μC_n , compound concentration corresponding to each tracer, kg/m³; M , dosage of tracer compound in each section, kg; V_T , total volume of fracturing fluid pumped into the formation, m³; V_E , volume of fracturing fluid pumped into the formation in each section, m³; N , number of fracturing sections; P_T , maximum discharge capacity of the fracturing truck, m³/min; and T , time required for each stage of fracturing, min.

μ is a dimensionless correction coefficient that incorporates factors such as formation water intrusion and coal seam adsorption. Its value can be determined by $\mu = D_W \times A_t \times N \times$

T_r , where D_W is the fold of considering formation invasion, dimensionless; A_t is a fold considering the multiple of coal seam adsorption, dimensionless; N is the number of stages of staged fracturing; and T_r is the fold of the tracer retention time in the formation, dimensionless.

We also determined the discharge capacity of the metering pump according to the different solubility levels of each tracer compound. Assuming that the solubility of the tracer compound is X (kg/L), the water volume V_T required to dissolve the tracer compound in each section can be obtained. The discharge capacity P of the metering pump can then be calculated according to the fracturing time t of each section as shown in eqs 4 and 5.

$$V_W = M / X \quad (4)$$

$$P = 60V_W / T \quad (5)$$

V_W , volume of solution prepared by each tracer compound, L; X , solubility of tracer compound, kg/L; and P , discharge capacity of the metering pump, L/h.

In this block, Well B8-3P7 and Well B8-3P8 are the dual tracer injection wells. The tracer dosage required for each fracturing section of the two wells was calculated according to the fracturing design of the two wells combined with the characteristics of the tracers. The dosage design for the two tracer injection wells is shown in Figure 8.

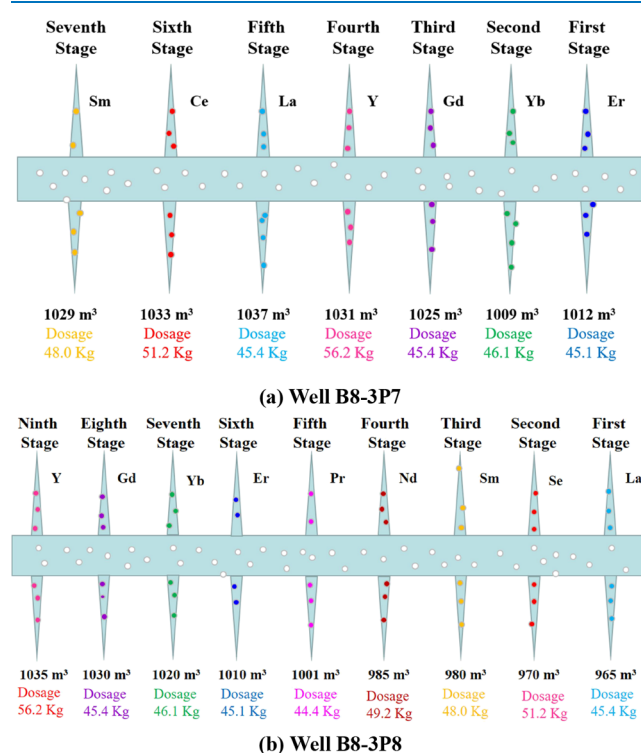


Figure 8. Dosing of micromaterial tracers.

2.5.3. Monitoring and Analysis of Tracers in Adjacent Wells. A trace material tracer staged fracturing test was carried out for B8-3P7 and B8-3P8 horizontal wells. The flowback fluid of two test wells and four adjacent wells (Well B8-3P6, Well B8-4P2, Well B8-4P1, and Well B8-3P5) was sampled and monitored. The tracer test results of two adjacent wells (Well B8-4P2 and Well B8-3P5) are shown in Figure 9. Adjacent well B8-4P2 began to flow back during tracer

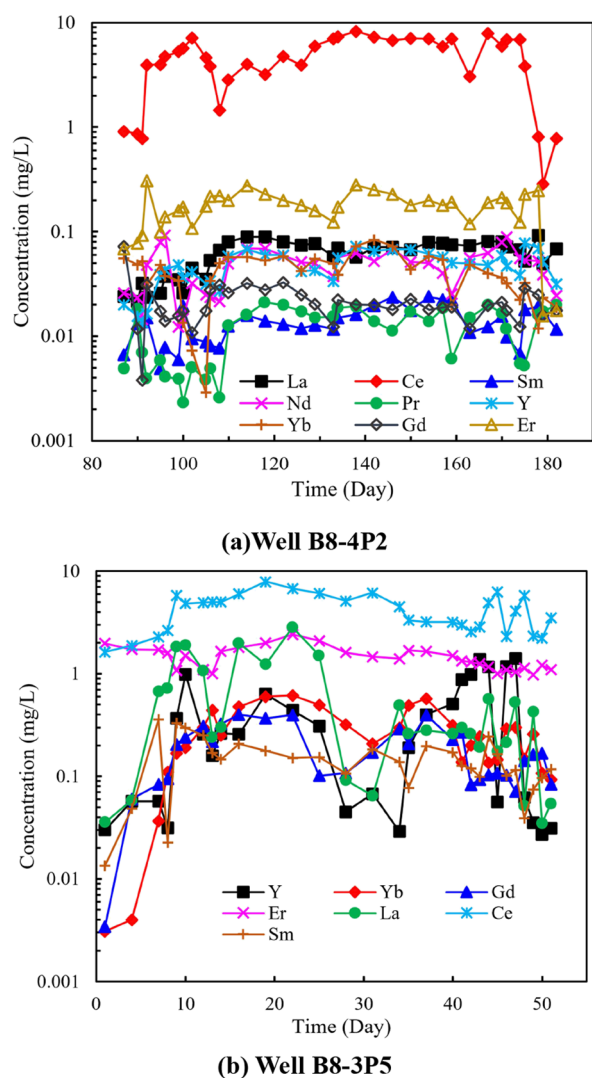


Figure 9. Trace material tracer dynamic of the production well.

fracturing, which continued for about three days, then did not flow back again until 80 days later during the drainage and gas production stage. Well B8-3P5 did not flow back during the tracer fracturing construction stage of the two wells, but started to flow back in the drainage and gas production stage.

Tracer elements were detected in the two distant adjacent wells to varying extents. The detection results of the two wells share a common feature wherein the content of one tracer element is very high (Ce element in Well B8-4P2; Ce element in Well B8-3P5), although the detected contents of the remaining tracer elements are negligible. Because the fracturing layer corresponding to the Ce element in the two wells is the interbedded layer of semi-bright coal and bright coal, while the other layers are single coal seams or containing calcareous gangue, we speculate that the reservoir of the interbedded layer of bright coal and semi-bright coal is more conducive to the extension of cracks. Furthermore, we infer that the sixth level corresponding to the Ce element in the B8-3P8 well and the sixth level corresponding to Ce in the B8-3P7 well are the dominant seepage channels.

Although the two adjacent wells show different peaks at different times, their monitoring curves do show three obvious peaks. The formation of the first peak is attributable to the accumulation of tracer seepage. The interval is around 80 days

as per the fracturing operation process. In this interval, the tracer continued diffusing into the surrounding adjacent wells along the seepage channel. When the two adjacent wells entered the drainage gas production stage and began to produce flowback fluid, the tracer concentration in the flowback fluid was naturally high and then gradually decreased. As the formation pressure decreased, the tracer in each fracturing section began to gradually discharge. The tracer content of each section monitored by adjacent wells was also different due to the different fracturing effects and physical properties of each section. The tracer may have encountered blockages in the process of diffusion along the seepage channel. As per the distribution of the peaks in Figure 9, blockages were indirectly cleared with the accumulation of time and fluid flow, resulting in the occurrence of these peaks.

Well B8-4P2 and Well B8-3P5 were regarded as two tracer injection wells in this experiment. Tracers were detected in the flowback fluid indicating that fractures from Well B8-3P7 and Well B8-3P8 connected surrounding adjacent wells. The spacing between the horizontal wells drilled in the B8-3 block is between 300–330 m. According to the existing tracer monitoring results, each well was connected to far-away neighboring wells after staged fracturing (Figure 10),

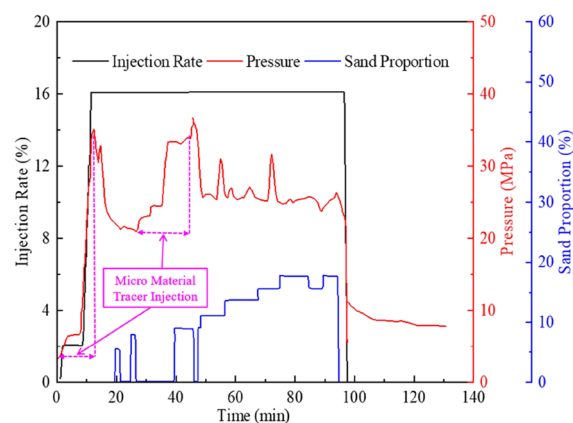


Figure 10. Fracturing dynamics of Well B8-3P7.

suggesting that the spacing between the existing horizontal wells was too small. From an economic and reservoir development perspective, the spacing should be increased to 400–450 m.

2.5.4. Existing Problems and Analysis. We find that during the fracturing operation, the casing pressure increased rapidly after the trace material tracer solution (including chemical agent) was added. We conducted a simple test during the construction process to test the effects of tracer addition on the casing pressure during fracturing: We intermittently dosed (10 min on/off intervals) tracer agents and observed whether the casing pressure changed. We find that casing pressure continued to rise to about 38 MPa in the fracturing fluid after adding the tracer agent; after the dosing was stopped, the casing pressure decreased rapidly to about 25 MPa.

The sand-carrying ratio of the fracturing fluid also affects the casing pressure; casing fracturing increases when the sand-carrying ratio of the fracturing fluid is high. In our case, when the sand-carrying ratio was about 8%, the casing pressure was stable at about 22 MPa after the dosage is stopped. When the sand-carrying ratio was about 12%, the casing pressure was stable at about 26 MPa after the dosage was stopped. Small

Table 4. Formation Water in the Field-Study Block

ion	Na ⁺	K ⁺	Ca ²⁺	Mg ²⁺	Cl ⁻	SO ₄ ²⁻	HCO ₃ ⁻	CO ₃ ²⁻	OH ⁻
concentration (mg/L)	523.6	71.9	253.6	96.4	1028.2	3.0	782.3	0.0	0.0

changes in the casing pressure in the diagram can also be attributed to changes in the proportion of sand carried by the fracturing fluid.

It is possible that due to the limitations of our field construction conditions, tracers and chemical agents were injected in the solid form and the field construction temperature was low. Therefore, trace substances tracers and chemical agents (EDTA, HDEHP, and NaOH) did not rapidly dissolve or dilute after injection, so the dissolved part produced a large amount of foam. Severe turbulence and increase in friction occurred in the pipe as the fracturing fluid was pumped into the formation at high speeds through the pipe string after being pressurized by the high-pressure pump. As a result, the casing pressure increased rapidly during the fracturing process. The ability of each rare-earth element to produce bubbles at the same concentration differs as well, so the pressure increase caused by the injection of different tracers differs.

The problematic increase in friction in the pipe due to the addition of tracers can be resolved by controlling the dosage of tracers and friction reducers, and by the addition of antifoaming agents. If possible, it is also preferable to construct in summer months and avoid construction in winter (i.e., in low temperatures).

3. CONCLUSIONS

The trace material tracer is compatible with the fluid used for the fracturing of coal seams; the materials do not interfere with each other. The detection limit for the tracer is very low with high sensitivity, and there is no interference between trace substances and tracers. Due to the unique characteristics of coal, the adsorption loss of a trace substance tracer in the core porous surface is extremely high. However, the adsorption loss of the nine tracers we tested in this study exceeds the maximum adsorption loss required for field applications.

The EDTA + HDEHP + NaOH system we used in this study shows a strong inhibitory effect on the adsorption capacity of trace substance tracers. Field application requirements are met when the tracer concentration is higher than 800 C_n. Our field operation results demonstrate that trace material tracers can be used as fracturing tracers in staged fracturing tests of horizontal wells in coal reservoirs. In the field, we also find that tracers and chemical agents produce a large quantity of dense bubbles that cause a rapid increase in casing pressure during fracturing. Furthermore, the spacing between the existing horizontal wells is too small. According to our tracer monitoring results, the well spacing should be increased to 400–450 m to maximize economic returns and reservoir development.

4. EXPERIMENTAL METHODS

4.1. Experimental Apparatus and Tracers. Experimental apparatus: MTQ200 Electronic Balance (0–200 g), purchased from Shenzhen Mobil Electronics Co., Ltd.; HH-1A Constant Temperature Water Bath (RT + 5–100 °C), purchased from Beijing Kewei Yongxing Instrument Co., Ltd.; YHAM300 Stirrer (100–1800 r/min), purchased from Shanghai Huaiyuan Industrial Co., Ltd.; ICP-MS/Agilent 7900 Inductive Coupled Plasma Mass Spectrometer (part

per trillion-part per million), purchased from Shanghai Zhuangrun International Trade Co., Ltd.; and YK-002 Vibrating Screen (10–200 mesh), purchased from Hengyu Machinery Equipment Co., Ltd.

Lanthanide tracers and additives: Yttrium chloride hexahydrate, lanthanum chloride hexahydrate, praseodymium chloride hexahydrate, neodymium chloride hexahydrate, samarium chloride hexahydrate, holmium chloride hexahydrate, erbium chloride hexahydrate, ytterbium chloride hexahydrate, and cerium chloride hexahydrate (all purely analytical). EDTA-4Na (referred to as EDTA here) and Di(2-ethylhexyl) phosphate (HDEHP). Coal samples taken from Baode Block.

4.2. Formation Water Analysis. The formation water (pH 7.6) was detected and analyzed, as shown in Table 4.

The total concentration of cations is 945.52 mg/L, the total concentration of anions is 1816.47 mg/L, the total salinity is 2761.99 mg/L, and the solution is weakly alkaline. Trace material tracers (yttrium, lanthanum, praseodymium, neodymium, samarium, holmium, erbium, ytterbium, and other lanthanide elements) were not detected in the water quality test, so lanthanide elements can be considered the tracer candidate.

4.3. Tracer Stability, Compatibility, Interference Test.

We used the static method and mass spectrometer detection to investigate stability, compatibility, and interference. The test instrument is an ICP-MS (Agilent 7900; Shanghai Zhuangrun International Trade Co., Ltd.). We first configured a trace material tracer solution with a certain concentration and let it stand for 1–2 weeks. Samples were then taken for a concentration test on the mass spectrometer. First, we stabilized the room temperature to 18–26 °C while ensuring the change rate was less than 1 °C. After 30 min of plasma ignition, the instrument was standardized and a standard substance solution containing the representative elements was introduced into the plasma torch flame for 10 consecutive measurements. The relative error (RE) was calculated to test for accuracy.

4.4. Tracer Minimum Detection Limit Determination.

The minimum detection limit of the tracer was determined by the stepwise dilution method. The test instrument is an ICP-MS (Agilent 7900; Shanghai Zhuangrun International Trade Co., Ltd.). The tracer solution concentration was diluted step-by-step, and then the minimum detection limit of each indicator element was determined.

4.5. Tracer Static Adsorption Performance Test.

Coal samples were processed by first crushing, then sorting the coal into 10–16 mesh, 16–40 mesh, 40–60 mesh, and 60–80 mesh samples with a sieve. Mixed coal samples were used in the experiment. The mass ratio of 10–16 mesh, 16–40 mesh, 40–60 mesh, and 60–80 mesh coal samples was 1:1:3:7.

Fracturing fluid composed of water +1.0% NaCl +0.03% drag reducer +0.01% ammonium persulfate with a tracer concentration configuration of 50 C_n and the mixed solution (500 mL) were combined with the coal sample in a mass ratio of 1:1 and then left to stand for 14 days at a constant temperature of 43 °C. We sampled the mixture regularly to observe the amount of tracer adsorbed by the coal. We used the mass spectrometer detection method with an inductively

coupled plasma mass spectrometer (ICP-MS/Agilent 7900; Shanghai Zhuangrun International Trade Co., Ltd.).

4.6. Tracer Adsorption Performance Improvement Test. We obtained further test samples by subjecting the improved tracer solution to adsorption performance experiments. We detected tracer concentrations on an inductively coupled plasma mass spectrometer (ICP-MS/Agilent 7900; Shanghai Zhuangrun International Trade Co., Ltd.) which has measurement accuracy at the ppt level.

AUTHOR INFORMATION

Corresponding Authors

Wei Zhang – PetroChina Coalbed Methane Company Limited, Beijing 100028, China; orcid.org/0000-0003-2319-0153; Email: zhangwei2010@petrochina.com.cn

Lingbo Wang – PetroChina Coalbed Methane Company Limited, Beijing 100028, China; Email: wlb_cbm@petrochina.com.cn

Authors

Xiaoguang Sun – PetroChina Coalbed Methane Company Limited, Beijing 100028, China

Yongchen Li – PetroChina Coalbed Methane Company Limited, Beijing 100028, China

Gang Zhao – PetroChina Coalbed Methane Company Limited, Beijing 100028, China

Wenhui Meng – PetroChina Coalbed Methane Company Limited, Beijing 100028, China

Complete contact information is available at: <https://pubs.acs.org/10.1021/acsomega.2c06542>

Notes

The authors declare no competing financial interest.

REFERENCES

- (1) Cheng, Y. G.; Lu, Y. Y.; Ge, Z. L.; Cheng, L.; Zheng, J. W.; Zhang, W. F. Experimental study on crack propagation control and mechanism analysis of directional hydraulic fracturing. *Fuel* **2018**, *218*, 316–324.
- (2) Hakso, A.; Zoback, M. The relation between stimulated shear fractures and production in the Barnett Shale: Implications for unconventional oil and gas reservoirs. *Geophysics* **2019**, *84*, B461–B469.
- (3) Shawn, M. Role of geophysics in unconventional-resource development on display at URTEC 2016. *Lead. Edge* **2016**, *35*, 910–910.
- (4) Gregory, K.; Mohan, A. M. Current perspective on produced water management challenges during hydraulic fracturing for oil and gas recovery. *Environ. Chem.* **2015**, *12*, 261–266.
- (5) Zhao, L. Q.; Chen, Y. Y.; Du, J.; Liu, P. L.; Li, N. Y.; Luo, Z. F.; Zhang, C. C.; Huang, F. H. Experimental study on a new type of self-propping fracturing technology. *Energy* **2019**, *183*, 249–261.
- (6) Cao, D. S.; Zeng, L. B.; Lv, W. Y.; Xu, X.; Tian, H. Research progress on evaluation and prediction methods of unconventional reservoir brittleness. *J. Pet. Sci. Bull.* **2021**, *6*, 31–45.
- (7) Warpinski, N. R.; Wolhart, S. L.; Wright, C. A. Analysis and prediction of microseismicity induced by hydraulic fracturing. *SPE J.* **2004**, *9*, 24–33.
- (8) Luo, S. G.; Zhao, Y. L.; Zhang, L. H.; Chen, Z. G.; Zhang, X. Y. Integrated simulation for hydraulic fracturing, productivity prediction, and optimization in tight conglomerate reservoirs. *Energy Fuels* **2021**, *35*, 14658–14670.
- (9) Yu, T.; Guan, G. Q.; Wang, D. Y.; Song, Y. C.; Abuliti, A. Gas production enhancement from a multilayered hydrate reservoir in the south china sea by hydraulic fracturing. *Energy Fuels* **2021**, *35*, 12104–12118.
- (10) Mayerhofer, M. J.; Lonon, E. P.; Warpinski, N. R.; Cipolla, C. L.; Walsler, D. What is stimulated rock volume? *C. SPE Shale Gas Production Conference*, 2008. SPE-119890-MS.
- (11) Asadi, M.; Shook, G. M. Application of Chemical Tracers in IOR: A Case History. *SPE J.* **2010**, DOI: [10.2118/126029-MS](https://doi.org/10.2118/126029-MS).
- (12) Wang, J. C.; Li, H. T.; Wang, Y. L.; Jiang, B. B.; Luo, W. A new model to predict productivity of multiple-fractured horizontal well in naturally fractured reservoirs. *Math. Probl. Eng.* **2015**, *2*, 1–9.
- (13) Guk, V.; Tuzovskiy, M.; Wolcott, D.; Mach, J. Optimizing the number of fractures in a horizontal well. *SPE J.* **2019**, *24*, 1364–1377.
- (14) Kissinger, A.; Helmig, R.; Ebigbo, A.; Class, H.; Lange, T.; Sauter, M.; Heitfeld, M.; Klünker, J.; Jahnke, W. Hydraulic fracturing in unconventional gas reservoirs: risks in the geological system, part 2. *J. Environ. Earth Sci.* **2013**, *70*, 3855–3873.
- (15) Zhao, J.; Zhao, J. Z.; Hu, Y. Q.; Zhang, S. A.; Liu, X. J. Numerical simulation of multistage fracturing optimization and application in coalbed methane horizontal wells. *Eng. Fract. Mech.* **2020**, *223*, No. 106738.
- (16) Wang, H.; Liao, X.; Ding, H. Monitoring and evaluating the volume fracturing effect of horizontal well. *J. Nat. Gas Sci. Eng.* **2015**, *22*, 498–502.
- (17) Ruan, L. H.; Wang, L. S.; Wu, J.; Lu, X. H. Research and application of horizontal well testing technology for heavy oil thermal recovery. *J. Pet. Technol. Forum* **2009**, *28*, 43–46.
- (18) Tang, H. W.; Hasan, A. R.; Killough, J. Development and application of a fully implicitly coupled wellbore/reservoir simulator to characterize the transient liquid loading in horizontal gas wells. *SPE J.* **2018**, *23*, 1615–1629.
- (19) Song, W. G.; Jia, N.; Jiang, Q. Q. An Interpretation model for the production profile on the same angle of a horizontal well trajectory. *Front. Energy Res.* **2020**, *8*, 203.
- (20) Ji, B. Y.; Sui, X. G.; Wang, Q. L.; Li, Q.; Liu, A. J.; Liu, T. J. Advance on the tracer test technology among wells. *J. Isotopes* **2007**, *20*, 189–192.
- (21) Li, P. P.; Zhang, X. D.; Zhang, S. Structures and fractal characteristics of pores in low volatile bituminous deformed coals by low-temperature N₂ adsorption after different solvents treatments. *Fuel* **2018**, *224*, 661–675.
- (22) Pan, J. N.; Hou, Q. L.; Ju, Y. W.; Bai, Y. Q.; Zhao, Y. Q. Coalbed methane sorption related to coal deformation structures at different temperatures and pressures. *Fuel* **2012**, *102*, 760–765.
- (23) Nie, B. S.; Liu, X. F.; Yang, L. L.; Meng, J. Q.; Li, X. C. Pore structure characterization of different rank coals using gas adsorption and scanning electron microscopy. *Fuel* **2015**, *158*, 908–917.
- (24) Li, P. P.; Zhou, S. X.; Zhang, X. D.; Li, J.; Zhang, S.; Hou, A. Q.; Guo, C. Analysis on correlation between nanopores and coal compositions during thermal maturation process. *Mar. Petrol. Geol.* **2020**, *121*, No. 104608.
- (25) Myers, M.; White, C.; Force, T. L.; Heath, C.; Gong, S.; Stalker, L.; Pejčić, B. The impact of partition coefficient data on the interpretation of chemical tracer behaviour in carbon geosequestration projects. *Chem. Geol.* **2017**, *465*, 52–63.
- (26) Yang, E. L.; Chen, C. Y.; Song, K. P.; Liu, M. J. Sieving inter well tracers for use in Southern District II of Daqing. *J. Oil-Field Chem.* **2007**, *24*, 12–16.
- (27) Gavrilenko, M. A.; Gavrilenko, N. A. Solid-phase extraction of fluorinated benzoic acids for the chromatographic analysis of oil tracer agents. *Mendeleev Commun.* **2015**, *25*, 159–160.
- (28) Hamidipour, M.; Mostoufi, N.; Sotudeh-Gharebagh, R.; Chaouki, J. Monitoring the particle-wall contact in a gas fluidized bed by rpt. *J. Powder Technol.* **2005**, *153*, 119–126.
- (29) Li, H. T.; Liu, Z. M.; Li, Y.; Luo, H. W.; Cui, X. J.; Nie, S.; Ye, K. R. Evaluation of the release mechanism of sustained-release tracers and its application in horizontal well inflow profile monitoring. *ACS Omega* **2021**, *6*, 19269–19280.

- (30) Yang, D. Y.; Cui, H. W.; Zhang, Q.; Li, L. H.; Wu, Z. Tracer for Water-Alternating-Gas Miscible Flooding in Pubei Oil Field. *SPE J.* **2000**, SPE-62847-MS.
- (31) Serres-Piole, C.; Commarieu, A.; Garraud, H.; Lobinski, R.; Preud'homme, H. New Passive Water Tracers for Oil Field Applications. *Energy Fuels* **2011**, *25*, 4488–4496.
- (32) Silva, M.; Bjrnstad, T. Determination of phase-partitioning tracer candidates in production waters from oilfields based on solid-phase microextraction followed by gas chromatography-tandem mass spectrometry. *J. Chromatogr. A.* **2020**, *1629*, No. 461508.
- (33) Asadi, M.; Woodroof, R. A.; Himes, R. E. Comparative study of flowback analysis using polymer concentrations and fracturing-fluid tracer methods: A Field Study. *SPE Prod. Oper.* **2008**, *23*, 147–157.
- (34) Serres-Piole, C.; Preud'homme, H.; Moradi-Tehrani, N.; Allanic, C.; Jullia, H.; Lobinski, R. Water tracers in oilfield applications: Guidelines. *J. Pet. Sci. Eng.* **2012**, *98*, 22–39.
- (35) Valestrand, R.; Sagen, R.; Naevdal, R.; Huseby, R. The effect of including tracer data in the ensemble-kalman-filter approach. *SPE J.* **2010**, *15*, 454–470.
- (36) Kumar, A.; Seth, P.; Shrivastava, K.; Manchanda, R.; Sharma, M. M. Integrated analysis of tracer and pressure-interference tests to identify well interference. *SPE J.* **2020**, *25*, 1623–1635.
- (37) SY/T 5925–2012, Selection method of chemical tracer for oilfield water injection. S. SY/T 5925-2012
- (38) Chang, Q.; Li, Q. Y.; Zhao, P.; Cai, J. P.; Cao, X. X.; Li, S.; Zhou, X.; Shao, S. Development of lanthanide metal tracers and their application in Sulige area. *J. Drill. Fluid Compl. Fluid.* **2018**, *35*, 114–118. +123